Clays Clay Miner. (2023) 71:559–576
https://doi.org/10.1007/s42860-023-00258-0

ORIGINAL PAPER

Antibacterial finishing of textile materials using modified bentonite

Ljiljana Topalić-Trivunović · Aleksandar Savić · Rada Petrović · Darko Bodroža · Dragana Grujić · Miodrag Mitrić · Zoran Obrenović · Dragana Gajić · Mugdin Imamović

Accepted: 5 October 2023 / Published online: 6 November 2023

Abstract Direct application of heavy metals as antibacterial agents can cause skin irritations and discoloration of the tissue and it can result in short-term applicability. One of the ways to solve these problems is to immobilize these agents on bentonite. Treatment of textile materials with such activated bentonite for use in various branches of industry has attracted the attention of many researchers in recent years. The objective of the present study was to develop a potential use of Cu- and Zn-modified bentonites as antibacterial finishing agents for two textile materials, non-woven textile (NT) and knitted fabric (PL). The bentonite samples were characterized using ED-XRF (energy dispersive X-ray fluorescence spectrometry), XRPD (X-ray powder diffraction), SEM (scanning electron microscopy), FTIR (Fourier-transform infrared spectroscopy), and BET (N_2 adsorption-desorption) analyses. SiO_2 and Al_2O_3 oxides were the main components of all bentonite samples indicated by ED-XRF analysis, while the XRPD analysis confirmed that the natural bentonite (NB) consisted of montmorillonite (Mnt) as the dominant mineral (peaks at 6.94, 19.94, 35.09, and 54.09°2θ) and small amounts of quartz and calcite. A reduction in the basal plane spacing, d_{001}, of Mnt occurred in Cu/Zn-B1, Cu/Zn-B3, and CuB, while in Cu/Zn-B2 and ZnB the basal spacing increased. Also, the size and form of particles and porosity changed, which was confirmed by the BET analysis. Modified bentonite samples experienced a reduction in the specific surface area and total pore volume, as well as movement of the middle mesopore diameter toward the larger diameters. The Zn-modified bentonite demonstrated a greater antibacterial effect on *Escherichia coli*, *Pseudomonas aeruginosa*, *Staphylococcus aureus,* and *Bacillus cereus* than Cu- and Na-modified bentonite samples with a MIC (minimum inhibitory concentration) of 0.94 mg/mL, while among Cu/Zn bentonite samples, Cu/Zn-B2 had the strongest antibacterial effect (MIC 0.47 mg/mL). Cu/Zn-B2 was integrated on NT and PL using a screen printing method and showed good antibacterial activity. The printed NT

Associate Editor: Chun-Hui Zhou

L. Topalić-Trivunović · A. Savić (✉) · R. Petrović · D. Bodroža · D. Grujić
University of Banja Luka, Faculty of Technology, Banja Luka, Bosnia and Herzegovina
e-mail: aleksandar.savic@tf.unibl.org

M. Mitrić
Vinča Institute of Nuclear Sciences, University of Belgrade, Belgrade, Serbia

Z. Obrenović
University of East Sarajevo, Faculty of Technology, Zvornik, Bosnia and Herzegovina

D. Gajić
University of Banja Luka, Faculty of Natural Sciences and Mathematics, Banja Luka, Bosnia and Herzegovina

M. Imamović
Cement Factory Lukavac, Lukavac, Bosnia and Herzegovina

showed better activity than printed PL, and increasing the concentration of applied Cu/Zn-B2 also increased the antibacterial properties.

Keywords Antibacterial finishing · Characterization · Modified bentonite · Multifunctional textile

Introduction

Microbial contamination of the air, water, soil, and, therefore, of food represents a serious health problem, especially due to an increased number of bacteria that are resistant to antibiotic drugs. This is why materials with antimicrobial properties, which might help solve this problem, are being tested. These materials include activated aluminosilicates such as bentonite, which are generally used in industrial processes mostly due to their good adsorption properties. Antibacterial clays are those that are shown explicitly to diminish bacterial populations, as opposed to bacteriostatic substances that simply prevent growth (Williams, 2019). In the biomedical field, some clay minerals, such as halloysite (Hly) and montmorillonite (Mnt), are known for their effective role as carriers for the control and sustainable delivery of active drug molecules. In the biomaterials field, some clay minerals are used for scaffold, hydrogel, foam, and film production (Gomes et al., 2021). Modified natural bentonite (NB) and Mnt were used as fillers in the modification of polymer materials such as polyethylene, polypropylene, polystyrene, and nylon by Abou el-Kheir et al. (2020), Roy and Joshi (2018), and Uddin (2013). Those authors noticed that, in addition to the demonstrated antimicrobial effect, mechanical and thermal properties, flame resistance (peak heat release rate), UV protection, and dyeability were improved also. Montmorillonite was modified (Stodolak-Zych et al., 2021) with gentamicin sulfate, which improved the strength and tenacity of electrospun polycaprolactone fibers and prolonged the antimicrobial effect, while Bhattacharya et al. (2008) and Sadhu and Bhowmick (2004) prepared organomodified Mnt with improved mechanical properties of a rubber polymer. A novel treatment based on Hly nanotubes and Keratin mixtures for wool threads was proposed by Caruso et al. (2023). The results of their study showed that Hly nanotubes can be glued to the surface of wool fiber, causing the scales to act as an anchoring site for the threads. A novel protocol for the loading of Hly nanotubes with an alkaline reservoir for the treatment of cellulose-based paper was designed by Lisuzzo et al. (2021). Dynamic mechanical analysis showed that the tensile strength of the consolidated paper is increased, as the stress at breaking increased by ~8% for the samples treated with MgO-Hly compared with untreated paper. In most of these experiments, however, complex and expensive procedures were used; simpler and cheaper procedures for modification are needed.

The main component of bentonite is Mnt, which imparts important properties to the system, including a high cation exchange capcity (CEC), speific surface area, and surface hydration forces. According to Gamiz et al. (1992) and Aguzzi et al. (2007): not only because of their large CEC, surface area, and swellability, but also because of their biocompatibility, clay minerals have been recommended frequently for biomedical applications, especially pharmaceuticals.

In the area of antimicrobial protection, Mnt exchanged with Ag^{+}, Ca^{2+}, Mg^{2+}, Cu^{2+}, Zn^{2+}, quaternary ammonium and anionic surfactants, hexadecyltrimethylammonium, and chlorhexidine diacetate have been identified as having antimicrobial properties (Bagchi et al., 2013; Parolo et al., 2011; Pazourková et al., 2019; Şahiner et al., 2022). Cu^{2+}- and Zn^{2+}, in particular, have exhibited strong antibacterial effects (Abdalkader & Al-Saedi, 2020; Benhalima et al., 2019; Paetzold & Wiese, 1975; Rather et al., 2020; Söderberg et al., 1990; Surjawidjaja et al., 2004). These ions interfere with the synthesis, structure, and porosity of the bacterial cell wall and membrane. They bind to proteins and inhibit enzyme performance, which leads to an increase in reactive oxygen species which damage DNA and, thereby, prevent bacterial replication (Claudel et al., 2020; Hong et al., 2012; Ishida, 2017; Ning et al., 2015; Pourabolghasem et al., 2016; Sugarman, 1983).

In recent decades, the application of natural fibers and environmentally compatible processes for textile finishing and achieving of antibacterial properties in textile materials have become increasingly popular due to ecological concern and environmental safety (Benli & Bahtiyari, 2015; Hasan et al., 2016; Joshi et al., 2009). Application of clay mineral nanocomposites by direct coatings as a simple, fast, and cheap method has been investigated mostly for testing the

https://doi.org/10.1007/s42860-023-00258-0 Published online by Cambridge University Press

thermal stability of various textile fibers and materials (de Oliviera et al., 2021; Kertman et al., 2020). Silver-modified Mnt, bentonite (84% Mnt), and Cloisite®Na^+, applied by different methods on cotton, bacterial cellulose, and starch-based matrix, showed a significant inhibitory effect on the growth of *S. aureus*, *K. pneumoniae*, *E. coli*, *P. aeruginosa,* and *K. rhizophila*, and on the fungus *A. niger* (Begam et al., 2022; Clegg et al., 2019; Horue et al., 2020). These studies described the antimicrobial effect of materials coated with silver-modified Mnt as being due to the release of silver ions, which are toxic to microorganisms. Also emphasized in these referenced studies was the need to use a technique that slows the rate and extent of release of the silver ions to prevent their accumulation and concomitant toxic effect on humans, especially when they are used for food packaging and wound treatment. In contrast, bentonite modified with copper and zinc does not display the negative properties of silver, and is cheaper (Martsouka et al., 2021). Pajarito et al. (2018) used zinc-modified bentonite as a filler for raw natural rubber and found good antimicrobial activity and intense reduction of offensive odor. Inorgano (I)- and organo (O)-Mnts (I/O-Mnt) were prepared by Şahiner et al. (2022) to determine their potential uses in biomedical applications. Those authors modified Na-Mnt by hydrothermal and microwave irradiation methods using Cu^{2+}/Zn^{2+} and quaternary ammonium and/or anionic surfactants. Their antibacterial studies showed that the linear alkyl chain and a double aromatic ring were the structural factors causing the greatest antibacterial effect. Most of the frequently used methods for testing the antibacterial effect of natural and modified bentonite are disc diffusion or micro- and macro-dilution methods. In the current study, MIC (minimum inhibitory concentration) and MBC (minimum bactericidal concentration) were determined by the agar dilution method (Magana et al., 2008), which has been covered little in the available literature on bentonite.

Within this general context, the objective of the present contribution was to study systematically the preparation of antibacterial textiles using Cu- and Zn-modified bentonite, for their possible use in the food, pharmaceutical, clothing, and footwear industries. Two textile materials (non-woven textile (NT) and knitted fabric (PL)) were chosen for the current study. The coating of NT and PT textiles with Cu- and Zn-modified bentonite was expected to improve the moisture-adsorption behavior and antibacterial activity of the textiles, which would establish their potential use in the production of disposable protective coats and T-shirts that could be worn under other types of protective clothing.

Experimental

Materials and Reagents

The bentonite raw material (NB) was collected from a quaternary sedimentary basin situated in Sokolac which is located near Šipovo, in Bosnia and Herzegovina (44° 16′ 31.08″ N, 17° 2′ 21.12″ E). Non-woven textile (NT) with a surface mass of 37.00 g m^{-2}, made from 100% polyester yarns, and knitted fabric (PL) with a surface mass of 117.60 g m^{-2}, made from 100% viscose bamboo rayon (Dubicotton, Kozarska Dubica, Bosnia and Herzegovina) were used. All chemicals used were of analytical grade: NaCl, $CuSO_4 \cdot 5H_2O$, $ZnSO_4 \cdot 7H_2O$, methylene blue dye, $Na_4P_2O_7$, H_2SO_4, and Na-alginate were purchased from Lach-ner (Neratovice, Czech Republic). Nutrient agar (NA) and Muller–Hinton agar (MHA) were purchased from Liofilchem (Roseto degli Abruzzi, Italy). Antibiotic discs of erythromycin (15 µg), gentamicin (10 µg), ciprofloxacin (5 µg), and ampicillin (10 µg) were from the Mast Group (Bootle, UK). Twice-distilled (tdw) or demineralized water (dmw) from Water System Mihajlov (Srbobran, Serbia) was used for preparation of all solutions.

Preparation of Modified Bentonite Samples

NB was dried for 24 h at 60°C, ground, and sieved. A fraction with particle size <0.2 mm was used for further experiments. Modified bentonite samples were prepared by a partially modified method of Jiao et al. (2017). In short, Na-bentonite (NaB) was prepared by dispersion of 10.0 g of NB in 100 mL of 1 M NaCl solution (58.44 g NaCl/L dmw). The suspension was placed on an ARE 5 magnetic stirrer (Velp Scientifica, Usmate, Italy) and stirred for 24 h at room temperature (600 rpm), filtered through a Büchner funnel, and the filter cake was rinsed with dmw until a negative reaction to Cl^- ions occurred. The NaB obtained was dried for 24 h at 60°C, ground, and

https://doi.org/10.1007/s42860-023-00258-0 Published online by Cambridge University Press

sieved to the particle size <0.2 mm. Cu-bentonite (CuB), Zn-bentonite (ZnB), and Cu/Zn-bentonite samples were prepared by dispersion of 10.0 g NaB in 100 mL of: 1 M $CuSO_4$ solution (249.685 g $CuSO_4 \cdot 5H_2O$/L dmw), 1 M $ZnSO_4$ solution (287.547 g $ZnSO_4 \cdot 7H_2O$/L dmw), and 1 M of mixed $CuSO_4$ and $ZuSO_4$ solutions, in ratios of Cu:Zn = 1:1, 1:2, or 1:4, respectively. Suspensions were placed on the ARE 5 magnetic stirrer and stirred for 24 h at room temperature (600 rpm), then sieved through a Büchner funnel. Upon rinsing with dmw multiple times, the filter cake was dried for 24 h at 60°C, ground, and sieved to the particle size <0.2 mm. Modified bentonite samples with $CuSO_4$ and $ZuSO_4$ solutions were marked: Cu/Zn-B1 (Cu:Zn = 1:1), Cu/Zn-B2 (Cu:Zn = 1:2), and Cu/Zn-B3 (Cu:Zn = 1:4), respectively.

Printing of Textile Materials with Selected Modified Bentonite Samples

Antibacterial treatment of the textile materials with selected modified bentonite was done using a printing process with a screen-printing semi-automatic machine S-300 (CENTRO MAŠINE, Sremski Karlovci, Serbia). Each sample of the textile material was printed in two passes with a 10 line sieve. The sieve line was determined by the granulation of the selected modified bentonite sample. The printing paste was prepared by adding Na-alginate and the selected modified bentonite sample in various percentages to dmw and mixing with a stick mixer until a homogeneous and consistent structure of the printing paste was achieved. Stereomicroscopic images of the textile materials were taken with 30× magnification using a TM-505 microscope (Mitutoyo, Kanagawa, Japan) and a high-resolution Moticam camera (5MP) (Motic, Hong Kong, China), before and after the printing process with paste containing various percentages of modified bentonite. Stereomicroscopy provides a good representation of changes on printed and dyed samples (Grujić et al., 2015; Amir et al., 2023; Wilson et al., 2023). The structures of the textile materials (non-woven textile (NT) and knitted fabric (PL)), the preparation of the printing paste, the printing process, as well as the labels and the appearance of the printed samples obtained using a stereomicroscope, are illustrated in Fig. 1.

Characterization of the Bentonite Samples

The methylene blue adsorption method was used for the determination of the cation exchange capacity (CEC) of NB (Aprile & Lorandi, 2012; Pejon, 1992). A methylene blue solution was prepared in a glass flask by adding 1.5 g of dye to 1 L of dmw and shaking thoroughly to obtain a homogeneous solution. 2 g of NB was placed in a 50 mL beaker containing 10 mL of dmw and stirred vigorously. The methodological assay began by adding 0.5 mL of the methylene blue solution to the beaker containing NB. After 3 min, a drop of the suspension material was removed with a glass rod and deposited on filter paper. When a light blue halo around the dark patch of NB appeared on the filter paper, the test was complete. Equation 1 was used to calculate the CEC:

$$\mathrm{CEC} = \frac{V \times C \times 100}{M} \quad (1)$$

where, CEC is in $mmol_c\ kg^{-1}$, V is the volume consumed of the methylene blue solution (mL), C is the concentration of the methylene blue solution, and M is the mass of dry NB (kg).

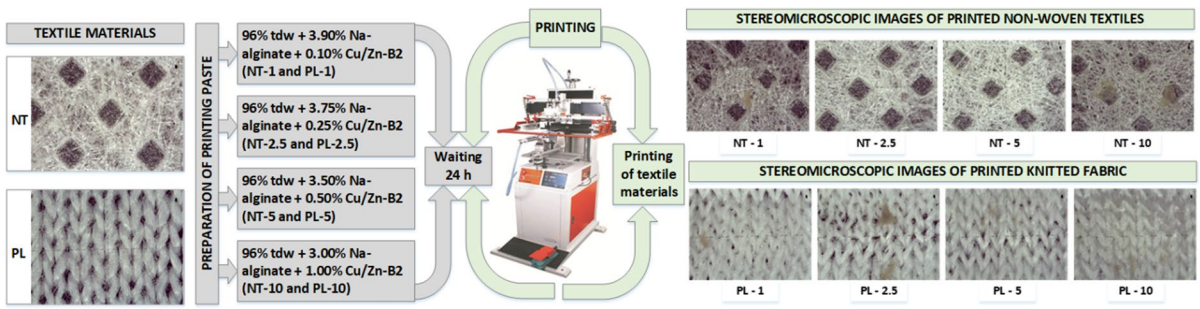

Fig. 1 The process of printing modified bentonite sample on textile materials

https://doi.org/10.1007/s42860-023-00258-0 Published online by Cambridge University Press

The methylene blue test was used for the quantification of Mnt content of NB (VDG P69, 1999). From the dried NB, 0.5 g was weighed on a KB 2400-2N balance (KERN & SOHN, Balingen, Germany) with an accuracy of 0.01 g and poured into an Erlenmeyer flask, to which 50 mL of dmw and 5 mL of a saturated solution of $Na_4P_2O_7$ had previously been added. The suspension thus prepared was boiled for 5 min, cooled, and 2 mL of 5 N H_2SO_4 was added and mixed for 30 s. The suspension was titrated with the methylene blue solution, and at the same time mixed vigorously for 2 min. With a glass rod, a drop of the suspension was deposited on filter paper until the end of the titration (a blue circle in turquoise blue color appeared around the solution on the paper). After the blue circle was detected, the solution was stirred in the flask for another 2 min and deposited again on filter paper. If the blue circle appeared again, then it was the end of the titration, and if it did not appear, the titration continued. Equation 2 was used for the calculation of the Mnt content in NB:

$$\%MM = \text{mL MB} \times 2 \quad (2)$$

where, $\%MM$ = Mnt content; mL MB = mL of methylene blue used for titration.

The chemical composition of the bentonite samples was determined by energy dispersive X-ray fluorescence spectrometry (ED-XRF) using an 8000P ED-XRF spectrometer (Shimadzu, Kyoto, Japan). The instrument was equipped with an X-ray tube with a rhodium anode. Measurements were performed at 50 kV and 1000 µA. A 10 mm collimator and silicon drift detector were used. The PCEDX *Navi* software was used for measurement and data processing.

The phase compositions of bentonite samples were determined by XRPD using a Bruker D4 Endeavor diffractometer (Billerica, Massachusetts, USA), using CuKα radiation (λ=0.1541 nm) operated at 40 kV and 35 mA over the range 4–60°2θ with a step size of 0.02°2θ.

The morphological properties of bentonite samples were recorded by scanning electron microscopy (SEM). Samples of 1 cm×1 cm size were stuck to the carrier across double-sided adhesive carbon tape and coated with gold in a BAL-TEC SCD005 device (Balzers, Liechtenstein) for cathode coating for 4 min from the distance of 50 mm, at 30 mA, which created a conductive surface. The recording was performed using JEOL JSM-5300 SEM (Tokyo, Japan). The observations were performed at an accelerating voltage of 20 kV. SEM analyses were performed with magnifications of 5,000× and 10,000×.

FTIR analysis of bentonite samples was performed using an IRSpirit ATR-FTIR spectrophotometer (Shimadzu, Kyoto, Japan) in the range from 4000 to 400 cm^{-1}. Specific surface area (SSA), total pore volume (Vp), and mean pore diameter (d) of bentonite samples were determined by N_2 physisorption at 77 K in a Gemini VII analyzer (Micromeritics, Norcross, Georgia, USA). The specific surface area (SSA) of the samples was calculated using the Brunauer–Emmett–Teller (BET) method (SP_{BET}). The total volume of mesopores, V_{mp}, as well as the mean diameter of mesopores, d_{mp}, were determined on the basis of the adsorption branch of the isotherm according to the BJH method (Barrett et al., 1951). The total micropore volume ($V_{micro,t}$), external specific surface area ($SP_{ext,t}$), and micropore surface area ($SP_{micro,t}$) were determined using the t-method (Lippens & de Boer, 1965). Prior to measurement, the samples were dried for 2 h at 200°C, then degassed for 1 h under a nitrogen stream at 140°C.

(level2) Determination of Water Absorption Capacity of Textile Fabrics (WAC)

The water absorption capacity of the textile materials was tested according to the standard DIN 53923:2022 DE (Testing of textiles–determination of the water absorption capacity of textile fabrics). Dry weight of fabric (10 cm×10 cm) was measured, then it was immersed in a bath of tdw for 5 min. Then, the fabric was hung vertically until no water droplet dripped for 30 s. At that time, the fabric was weighed again and the water absorption capacity was calculated using Eq. 3.

$$\text{Water absorption capacity (\%)} = \frac{wet\ weight - dry\ weight}{dry\ weight} \text{ x } 100\ (\%) \quad (3)$$

Antibacterial Activity

Four bacteria were used in this study: *Escherichia coli* ATCC 25922 (*E. coli)*, *Pseudomonas aeruginosa* ATCC 10145 (*P. aeruginosa)*, *Staphylococcus aureus* ATCC 25923 (*S. aureus)*, and *Bacillus cereus* ATCC 7004 *(B. cereus)*. The bacteria were grown on NA for 24 h at 37°C. After the incubation period, the colonies were prepared for application by a direct

https://doi.org/10.1007/s42860-023-00258-0 Published online by Cambridge University Press

suspension of colonies in the logarithmic phase (Ortez, 2005). Suspension density was determined spectrophotometrically (OD 625 nm) with spectrophotometer V-110 (Wagtech Projects, Thatcham, UK), using the 0.5 McFarland standard (1.5×10^8 cfu/mL) for comparison. The cultures were diluted in the physiological solution and their densities were set to 1×10^6 cfu/mL.

The antibacterial activity of the bentonite samples was determined by the agar dilution method with certain modifications (Magana et al., 2008). Before usage, the ground bentonite samples were sterilized for 30 min in a thin layer under the UV lamp (at 254 nm), then weighed under sterilized conditions and added to 2 mL of tdw. Bentonite was held in water at room temperature for 2 h, with occasional shaking, and a specific amount of melted MHA cooled at 50°C was added. The prepared medium was then homogenized and poured into sterile Petri dishes. The media obtained contained the following concentrations of the bentonite (in mg/mL): 0.94, 1.875, 3.75, 7.5, 15, 30, 60, and 100. After cooling the media, 10 µL drops of bacterial cultures were applied at the surfaces of all media and incubated for 24 h at 37°C. MIC values were determined in all the Petri dishes with the lowest concentration of the bentonite sample with no visible growth of microorganisms. All the Petri dishes without visible growth were loop-inoculated, in a way that all the spots containing drops of cultures were picked up with a sterile loop and transferred on sterile MHA. After incubating for 24 h at 37°C, the MBC values were read at MHA, where the growth of microorganisms was not spotted. As a positive control, the media without bentonite were used. As a first negative control, the salt solutions ($CuSO_4\cdot5H_2O$ and $ZnSO_4\cdot7H_2O$) in the agar medium were used, where the salt concentration was (in mg/mL): 0.25, 0.5, 1 2, 4, 8, 16, or 32. The other type of negative control was in the form of antibiotic discs (erythromycin 15 µg; gentamicin 10 µg; ciprofloxacin 5 µg, ampicillin 10 µg).

The antibacterial activity of the textile was tested by the Parallel Streak Method (AATCC TM 147-2004). Specimens of the test materials were placed in direct contact with the agar surface which had previously been streaked with an inoculum of a test bacterium. After incubation, a zone of inhibition (ZOI) (clear area of interrupted growth underneath and along the side of the test materials) was measured in mm. If a zone of inhibition was present, the streaks stopped at the edge of the sample and no growth was seen below the sample, it is defined as contact inhibition. This condition was defined as contact inhibition and the sample was reported as pass. Each measurement was determined in triplicate. After incubation, Eq. 4 was used to calculate the size of the zones of inhibition:

$$Zi = \frac{T - D}{2}\ (\text{mm}) \tag{4}$$

where, Zi = width of zone of inhibition, T = width of sample + zone of inhibition, D = width of sample (mm).

Results and Discussion

Characterization of Bentonite Samples

Natural bentonite (NB) from the Šipovo deposit in Bosnia and Herzegovina with an average particle size <0.2 mm was used. Mineralogical analysis revealed that the NB contained ~90% of Mnt (Eq. 1), with a CEC of 67.08 mmolM^+/100 g (Eq. 2).The chemical composition of NB and modified bentonite samples determined by the ED-XRF method (Table 1) revealed that Si and Al were the main components of NB, and a larger amount of Al was indicative of a higher concentration of Mnt. NB contained larger amounts of Fe and Mg, a medium amount of Ca, while K, Ti, and P were barely present. As NB does not contain Na, this type is classified as Ca-bentonite. The chemical analysis results of NB are in line with previously published results (Petrović et al., 2014, Petrović et al., 2019). Si and Al were the main components of NaB. Also, NaB contained more Fe and Na, medium amounts of Mg and Ca, while K, Ti, and S were barely present. Modification of NaB with copper and zinc ions caused the reduction of Ca, Mg, and K, and the complete absence of Na, which implies that an ion exchange occurred. The highest concentration of copper and zinc was found in Cu/Zn-B2. The adsorption behavior of the bentonite toward zinc and copper ions in aqueous solutions depends heavily on pH. When the pH is between 3 and 7, the basic mechanism that controls the adsorption properties of bentonite is ion exchange and specific adsorption (Aldayel et al., 2008; Kaya & Ören, 2005). The

https://doi.org/10.1007/s42860-023-00258-0 Published online by Cambridge University Press

Table 1 Chemical compositions of bentonite samples expressed as concentrations of metal oxides (in mass percentage)

Sample/Chemical composition (wt.%)	NB	NaB	CuB	ZnB	Cu/Zn-B1	Cu/Zn-B2	Cu/Zn-B3
SiO_2	58.84	58.48	47.79	50.15	50.05	34.02	37.56
Al_2O_3	27.48	24.87	21.50	24.69	22.62	17.51	20.69
Fe_2O_3	6.13	7.02	5.85	5.17	5.32	5.01	5.76
CaO	1.58	1.27	0.28	0.17	0.45	0.33	0.47
MgO	3.86	1.87	1.61	1.78	1.09	0.48	1.14
Na_2O	–	3.35	–	–	–	–	–
K_2O	0.35	0.32	0.25	0.27	0.26	0.18	0.17
TiO_2	0.69	0.81	0.65	0.64	0.64	0.60	0.64
SO_3	0.11	0.11	13.77	8.03	9.68	16.97	16.84
Cl^-	0.25	–	0.35	0.35	0.43	–	0.45
P_2O_5	0.33	–	0.02	0.02	–	–	–
Cr_2O_3	0.0.02	–	0.01	0.02	0.02	–	0.01
MnO	0.03	–	0.02	0.02	0.02	0.02	0.01
V_2O_5	0.11	–	0.11	0.10	0.10	0.04	0.08
Co_2O_3	0.13	–	0.13	0.14	0.13	–	0.12
Sc_2O_3	0.08	–	0.02	0.02	0.03	–	0.04
ZnO	–	–	–	8.41	4.17	16.27	12.29
CuO	–	–	7.59	–	4.98	8.56	3.72
Cu^{2+}	–	–	6.06	–	3.98	6.84	2.97
Zn^{2+}	–	–	–	6.78	3.35	13.07	9.87

concentration of TiO_2 in all bentonite samples was practically constant and showed that the Ti^{4+} cation is not exchangeable. A significant increase in the S concentration in the modified bentonite samples, in comparison to NaB, is the result of incomplete rinsing of the samples after modification.

XRD patterns of the modified bentonite samples (Fig. 2) revealed a diffraction peak at 7.16°2θ in the NaB, corresponding to d_{001} = 1.23 nm for Mnt. Upon modification with copper and zinc ions, the diffraction peak moved to higher angles of 7.08, 7.16, and 7.23°2θ (Cu/Zn-B1, Cu/Zn-B3, CuB, respectively), which corresponded to the smaller basal spacings of 1.25, 1.23, and 1.22 nm, respectively. As far as Cu/Zn-2 and ZnB are concerned, the reflection appeared at the lower angles of 6.84 and 6.64°2θ, respectively, which corresponded to an insignificant increase in the basal spacings to 1.29 and 1.33 nm, respectively. It is well known that bentonite consists mostly of Mnt. Modification of NaB with copper and zinc decreased the basal spacings of Cu/Zn-B1, Cu/Zn-B3, and CuB, but increased it for Cu/Zn-B2 and ZnB. Basal spacings of 1.24 and 1.34 nm

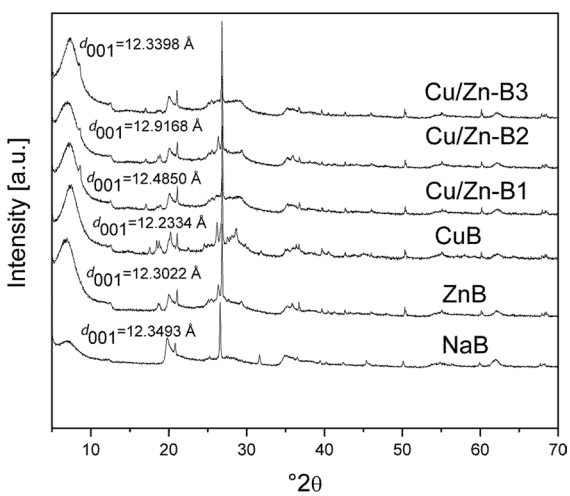

Fig. 2 XRD patterns of the bentonite sanples

for Cu- and Zn-Mnt, respectively, were reported by Kozák et al. (2010). The spacing depended on the initial concentration of the metal ion and the balance of pH, according to Németh et al. (2005). In the case of a large initial concentration of copper and

https://doi.org/10.1007/s42860-023-00258-0 Published online by Cambridge University Press

low pH; Cu-Mnt was reported to have a basal spacing of ~1.25 nm, which implied that the copper was inside the interlamellar space of Mnt with one layer of water. The basal spacing of Zn-Mnt increased progressively as the pH decreased, until it reached the permanent value of 1.40–1.50 nm at neutral pH, which implies that zinc has a tendency to exist with two layers of water inside the interlamellar space of Mnt. At lower pH, the interlayer zinc exists with two water layers. Bearing in mind the modification conditions of metal concentration and solution pH, the present results are in line with the results of Kozák et al. (2010), and are quite compatible with the results presented by Németh et al. (2005). The results of the XRPD analysis are an additional confirmation that, during the modification of NaB, the ion exchange of copper and zinc with exchangeable cations occurred.

To test the morphological properties of the bentonite samples, scanning electron microscopy (SEM) was performed. NaB showed the typical layered, loosely connected structure (Fig. 3) and, upon modification, no changes were observed in the layered structure or particle size and shape.

The FTIR spectra of the original and modified bentonite samples (Fig. 4) are almost identical. The octahedral Al^2O-H stretching vibration was observed at 3629 cm^{-1}, while the broad band at 3377 cm^{-1} (with CuB at 3169 cm^{-1}, and with ZnB at 3030 cm^{-1}), was ascribed to interlayer H_2O stretching modes (Farmer, 1974; Madejová, 2003; Russell & Farmer, 1964). The OH-bending modes were observed at 1637 cm^{-1}.

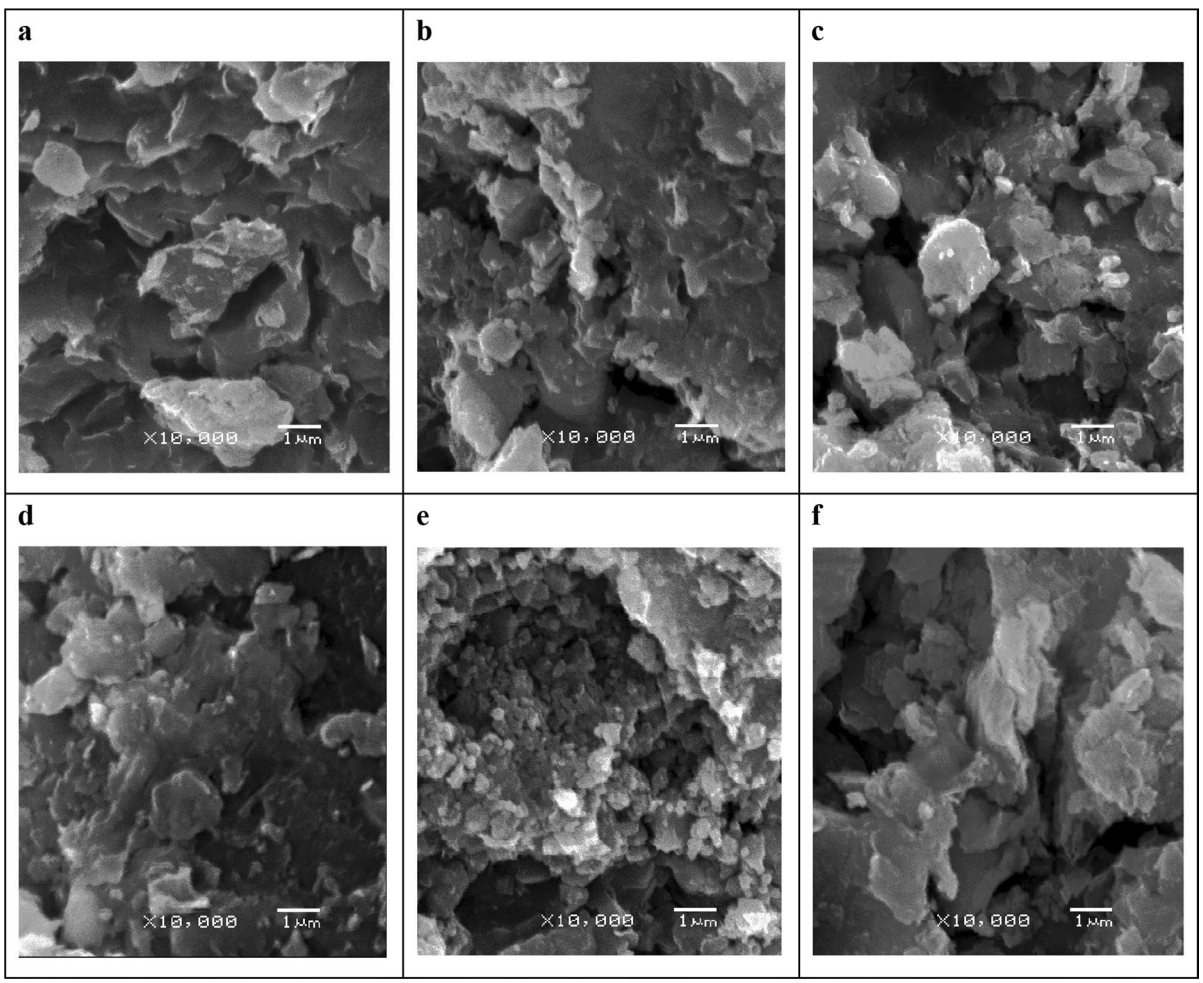

Fig. 3 SEM images of the bentonite samples: **a** NaB, **b** CuB, **c** ZnB, **d** Cu/Zn-B1, **e** Cu/Zn-B2, and **f** Cu/Zn-B3

https://doi.org/10.1007/s42860-023-00258-0 Published online by Cambridge University Press

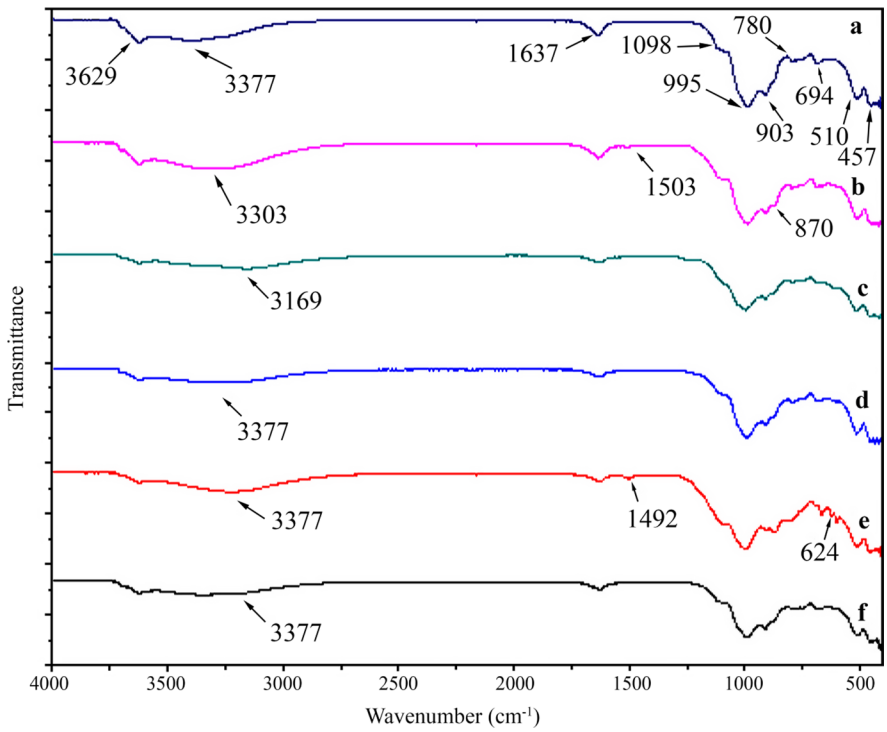

Fig. 4 FTIR spectra: **a** NaB, **b** ZnB, **c** CuB, **d** Cu/Zn-B1, **e** Cu/Zn-B2, and **f** Cu/Zn-B3

The bands at 1098 cm^{-1} and 995 cm^{-1} were the classical tetrahedral Si–O bands (Hayati-Ashtiani, 2012; Madejová, 2003). The bands corresponding to AlAlOH and AlFeOH bending modes which reflect a partial substitution of octahedral Al by Fe (Madejová, 2003; Tyagi et al., 2006), were observed at 903 and 870 cm^{-1}, respectively. The presence of quartz in the samples (which was proved by XRPD analysis) is indicated by the bands at 780 and 694 cm^{-1} (Ezquerro et al., 2015; Tyagi et al., 2006), while the bands at 510 and 457 cm^{-1} belong to AlOSi and SiOSi vibrations, respectively (Kumar & Lingfa, 2019; Madejová, 2003). The results for the most important textural properties of the bentonite samples, i.e. specific surface area (SP_{BET}), total pore volume (Vp), and middle pore diameter (d) (Table 2), showed that modification of NaB resulted in significant changes in textural properties, namely, reduction in the specific surface area and total pore volume as well as moving of the middle mesopore diameter toward the larger diameters. In comparison to NaB, the greatest reduction in the above-stated textural properties was with

Table 2 Overview of textural properties of bentonite samples

Textural properties	NB	NaB	CuB	ZnB	Cu/Zn-B1	Cu/Zn-B2	Cu/Zn-B3
SP_{BET} (m^2/g)	87.4990± 1.5759	56.1621± 0.5328	14.2651± 0.0347	6.5471± 0.0162	8.8641± 0.0075	35.4979± 0.2757	13.0326± 0.0213
V_{mp} (cm^3/g)	0.083908	0.079842	0.047057	0.023507	0.026468	0.051986	0.036856
d_{mp} (nm)	5.4810	6.6462	12.6883	13.4052	11.0955	6.4898	11.3363
$SP_{micro,t}$ (m^2/g)	16.4838	3.5427	0.9333	0.0658	0.1244	1.1631	0.4119
$SP_{ext,t}$ (m^2/g)	71.0152	52.6194	13.3318	6.4813	8.7398	34.3348	12.6207
$V_{micro,t}$ (cm^3/g)	0.009030	0.001723	0.000290	–0.000036	–0.000049	0.000468	0.000038

https://doi.org/10.1007/s42860-023-00258-0 Published online by Cambridge University Press

ZnB (SP_{BET} = 6.55 m^2/g, V_p = 0.023 cm^3/g, and d = 13.41 nm), and the smallest was with Cu/Zn-B2 (SP_{BET} = 35.5 m^2/g, V_p = 0.052 cm^3/g, and d = 6.49 nm). In all samples, the value of the $SP_{ext,t}$ was much greater than the $SP_{micro,t}$; $V_{micro,t}$ was small, and in the case of ZnB and Cu/Zn-B1 it even had a negative value (below the limit of detection). ZnB and Cu/Zn-B1 had the most pronounced mesoporous character, while NB had the least pronounced mesoporous character. The reduction of the SSA and the total pore volume could be attributed to the presence of copper and zinc cations in the interlamellar space and pores of bentonite which inhibited the passage of nitrogen molecules and their physisorption (de Araujo et al., 2013; Tan et al., 2008). Similar results were obtained with Mnt modified with zinc and zinc/cerium ions (de Araujo et al., 2013; Tan et al., 2008). Besides that, heat treatment could influence the clay textural properties. Prior to measurement, all bentonite samples were dried for 2 h at 200°C. The loss of mass in the temperature range 50 to 200°C corresponded to dehydration or the loss of physically adsorbed water and water connected to the exchangeable cations in the interlayer of aluminosilicate surfaces, which frequently led to a reduction in interlayer distances (Balek et al., 2008). The SSA of bentonite increased as the temperature increased to 100°C, but further increase in the temperature above 100°C caused the SSA to decrease (Toor, 2010). The increase in temperature above 100°C led to the removal of water connected to the exchangeable cations in the interlayer and to reduction of the interlayer distance. This reduction of the interlayer distance brought the particles closer and they started creating aggregates, which resulted in reduction of the specific surface area. The nitrogen adsorption isotherms for NB and modified bentonite samples (Fig. 5) and the structural properties estimated based on them (Table 2) revealed that all isotherms belong to the H type (IUPAC classification) (Balci, 2019; Jović-Jovičić et al., 2008; Ranđelović et al., 2014; Vuković et al., 2005). An isotherm of this type is characteristic of solid materials that can be non-porous, mesoporous, or even microporous to a certain extent. A small gas adsorption value corresponding to the micropore area (p/p_0 < 0.02) was observed in all of the isotherms, which

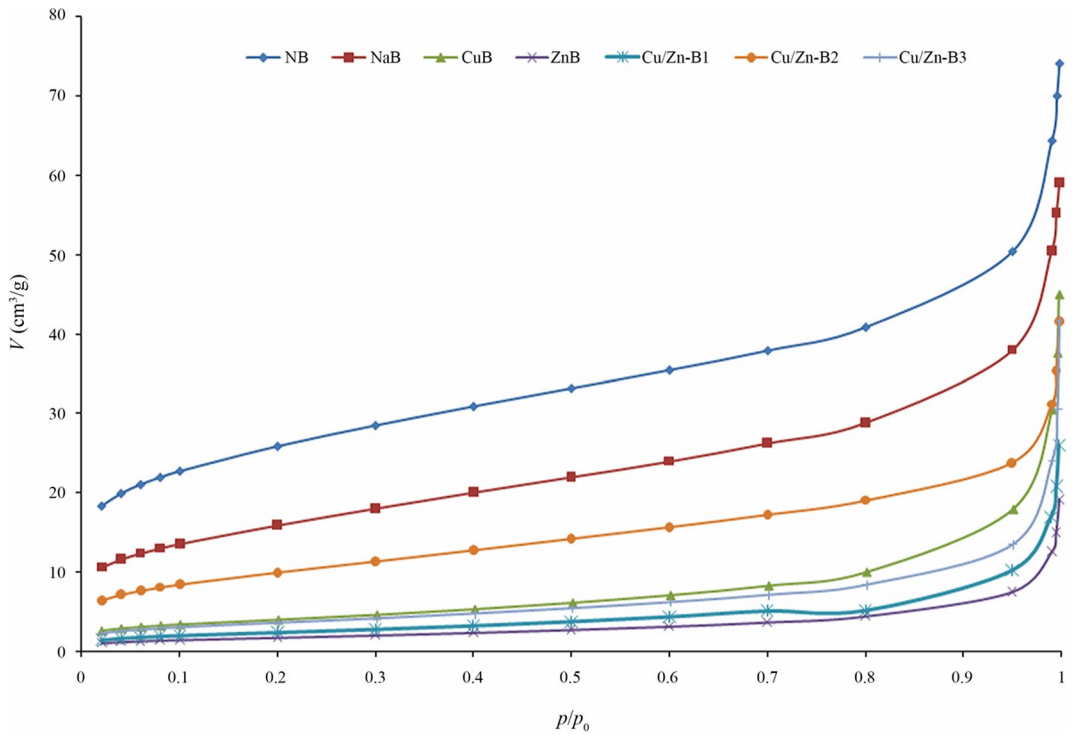

Fig. 5 Nitrogen adsorption isotherms for the bentonite samples

https://doi.org/10.1007/s42860-023-00258-0 Published online by Cambridge University Press

indicated a pronounced mesoporosity of the samples, and they all have steep slopes in the relative pressure range of 0.98–1.0. The modification process does not affect the type of isotherms obtained so one may conclude that the modification process did not affect the mesoporous character of the samples, but it led to significant changes in textural properties.

Determination of Water Absorption Capacity of Textile Materials (WAC)

The WAC is expressed as the amount of water absorbed (%) in the textile material after immersion in water at a temperature of 20°C. The WAC of the NT samples increased from 702.53 % (NT-1) to 865.27 % (NT-10) with increasing concentration of the modified bentonite in the paste (Table 3), thus proving the ability of modified bentonite to absorb large amounts of water. In the case of the PL samples, no clearly defined increase in WAC was observed. This can be explained by the yarn used in the PL samples which was obtained by the viscose process from bamboo and, thus, had a deformable structure that prevented the application of the bentonite in a precise thickness of the printing paste, whereas the opposite was true in the case of the NT samples.

Table 3 Results of testing of WAC (%)

Sample	Mean	Median	SD	Variance	p value
NT	220.35	220.43	0.83699	0.70055	0.19215
NT-1	702.53	703.02	0.74252	0.55133	0.03151
NT-2.5	731.41	731.30	0.63651	0.40515	0.76329
NT-5	815.30	814.91	0.79391	0.63030	0.27873
NT-10	865.27	865.36	0.28870	0.08335	0.49511
PL	315.85	315.78	0.69918	0.48885	0.98215
PL-1	520.71	518.69	4.40012	19.36105	0.16993
PL-2.5	512.41	511.39	3.44457	11.86505	0.87413
PL-5	503.44	503.79	2.06079	4.24685	0.96354
PL-10	548.11	549.39	4.70842	22.16925	0.32971

Antibacterial Activity

The MIC and MBC values of salts (as control) and bentonite samples (Table 4) showed that $CuSO_4 \cdot 5H_2O$ had good antibacterial activity. The antibacterial activity depended on the copper content, type of copper compound, temperature, pH, type of bacteria, etc. (Ahamed et al., 2014; Benhalima et al., 2019; Chen et al., 2016; Javadhesari et al., 2019). In comparison to $CuSO_4 \cdot 5H_2O$, $ZnSO_4 \cdot 7H_2O$ had a better inhibition effect on *S. aureus* and *E. coli* (MIC 0.5 and 1 mg/mL, respectively), and weaker on *B. cereus* and *P. aeruginosa* (MIC 2 and 4 mg/mL, respectively). Bacterial resilience in the presence of heavy metals depends on the type and concentration of metal, duration of exposure, type of bacteria, size of inocula, and other factors (Carpio et al., 2018; Henao & Ghneim-Herrera, 2021). NaB showed no antibacterial activity, while Cu^{2+}- and Zn^{2+}-modified bentonite showed antibacterial activity (but at different levels). The results obtained for NaB corresponded to the data available in the literature, where high concentrations of Na-Mnt had no inhibitory effect on bacterial growth (Bagchi et al., 2013; Jiao et al., 2017; Tong et al., 2005). The smallest MIC value (0.47 mg/mL) was established for Cu/Zn-B2 in

Table 4 MIC and MBC of salts and bentonite samples (mg/mL)

Bacterium/salt or bentonite sample	*S. aureus*		*B. cereus*		*E. coli*		*P. aeruginosa*	
	MIC	MBC	MIC	MBC	MIC	MBC	MIC	MBC
$CuSO_4.5H_2O$	1.00	2.00	1.00	4.00	1.00	2.00	2.00	2.00
$ZnSO_4.7H_2O$	0.50	1.00	2.00	4.00	1.00	1.00	4.00	8.00
NB	>100	>100	>100	>100	>100	>100	>100	>100
NaB	>100	>100	>100	>100	>100	>100	>100	>100
CuB	3.75	7.5	3.75	7.5	3.75	3.75	3.75	3.75
ZnB	0.94	1.875	7.5	7.5	1.875	3.75	7.5	15
Cu/Zn-B1	0.94	1.875	3.75	7.5	3.75	3.75	7.5	7.5
Cu/Zn-B2	0.47	0.94	1.875	7.5	0.94	0.94	3.75	3.75
Cu/Zn-B3	1.875	1.875	7.5	15	1.875	7.5	15	15

https://doi.org/10.1007/s42860-023-00258-0 Published online by Cambridge University Press

relation to *S. aureus,* while the largest MIC value (15 mg/mL) was established for Cu/Zn-B3 in relation to *P. aeruginosa*. Cu/Zn-B2 was applied to NT and PL due to the best antibacterial effect (Table 4). The Parallel Streak Method (ATCC TM 147) was used to test the antibacterial effect of textile samples treated with modified bentonite. With this technique, the antibacterial effect is manifested through the diffusion of the applied agent into the substrate and the appearance of a zone of inhibition or absence of bacterial growth under the sample. Untreated textile is used as a control sample (Figs. 6 and 7). Due to their surface topography and structure, NT and PL did not bind the tested bacteria or contain substances that have an antibacterial effect, or interfere with the formation of biofilms on the samples (Catovic et al., 2022; Ivankovic et al., 2022). The NT samples showed better antibacterial effects than PL samples (Figs. 6 and 7), because NT is a less porous and flat textile product, so more modified bentonite remained on the surface of the samples compared to PL, which is more porous, so the modified bentonite was incorporated between the threads within yarn. Due to the smaller amount of bentonite on the surface, PL had a weaker inhibitory effect on the growth of bacteria. The lack of an inhibition zone around the samples was expected considering the small desorption of Zn^{2+} and Cu^{2+} ions into the solid substrate, so the antibacterial action is localized on the surface of the modified bentonite (Hu & Xia, 2006; Pasquet et al., 2014), and occurs according to the mechanism that was previously described in the text. However, for both samples (Figs. 6 and 7), the inhibition of bacteria visibly increased with the concentration of applied modified bentonite. To test the survival of bacteria, the samples that were removed from the incubated media were again transferred to MHA and placed on the media on the side that was in contact with the bacteria, incubated for 24 h at 37°C, and removed from the media again. Much fewer bacteria were observed under the NT samples (Fig. 6), which can be explained by a larger amount of modified bentonite on their surface. Under the NT samples with modified bentonite in a concentration of >1 mg/mL, almost no bacterial

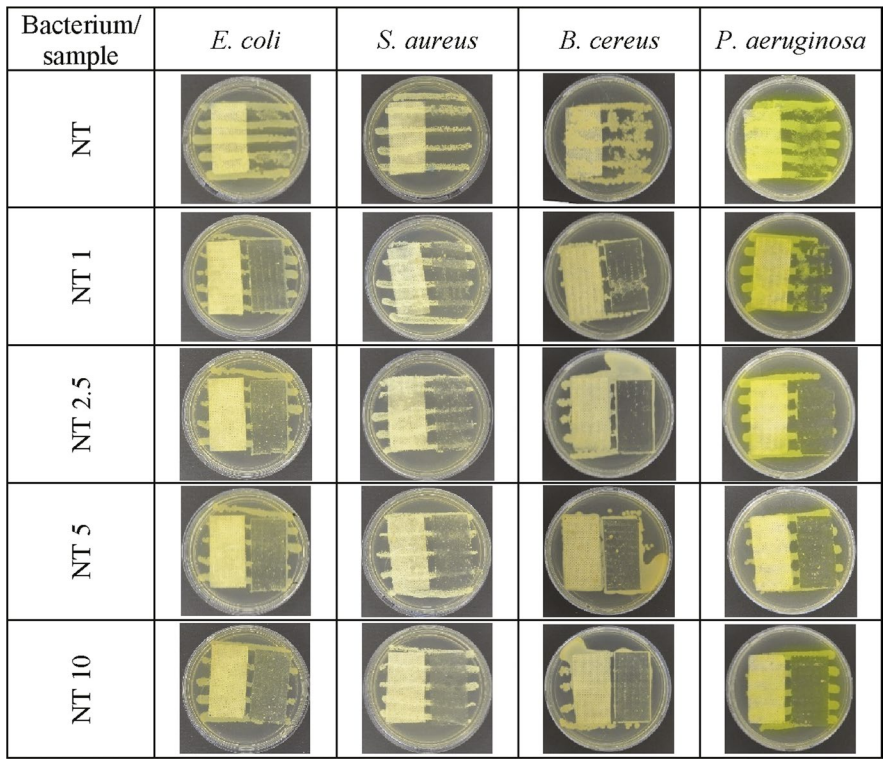

Fig. 6 Antibacterial activity of NT samples (right side of each petri dish indicates where the sample was removed from the agar plate)

https://doi.org/10.1007/s42860-023-00258-0 Published online by Cambridge University Press

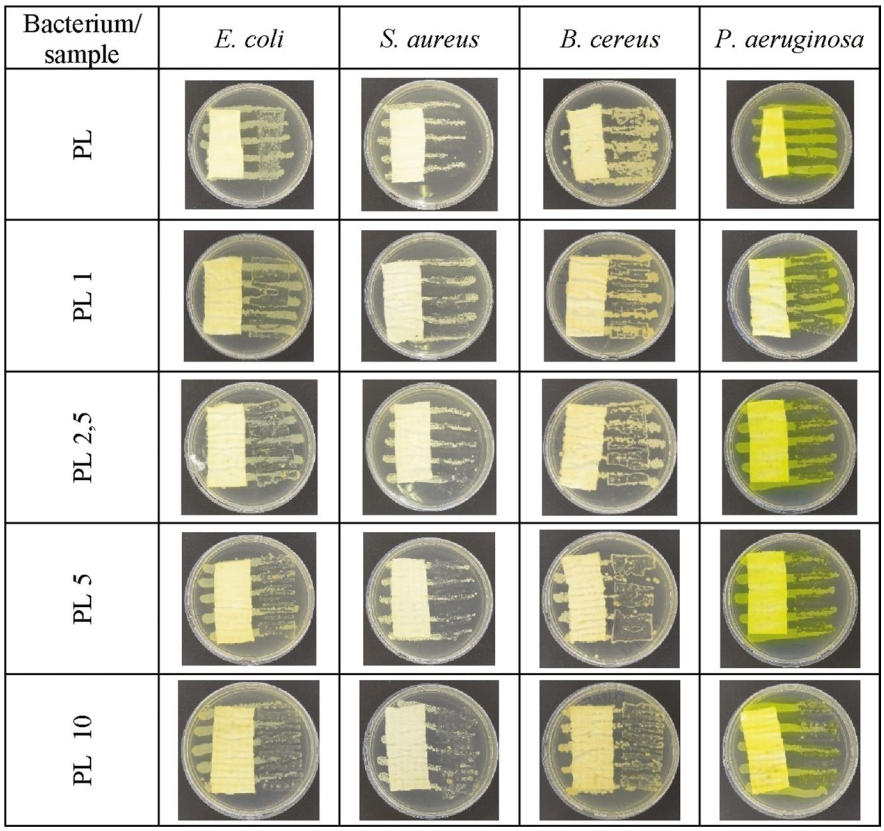

Fig. 7 Antibacterial activity of PL samples (right side of each petri dish indicates where the sample was removed from the agar plate)

growth occurred, indicating an outstanding bactericidal and bacteriostatic efficiency. The antibacterial effect of Cu- and Zn-modified Mnt is realized through direct contact of a negatively charged surface of bacterial cells and positively charged modified Mnt (Hu & Xia, 2006; Jiao et al., 2017; Kalia et al., 2020; Tong et al., 2005). Positively charged nanoparticles of metals connected to the cell membrane increased its permeability, therefore. Nanoparticles can also release metal ions which penetrate the cells and generate free radicals (Sanchez-Lopez et al., 2020). ZnB had a better antibacterial effect than CuB in relation to *S. aureus* (MIC = 0.94 mg/mL) and *E. coli* (MIC = 1.875 mg/mL), and weaker compared to *B. cereus* and *P. aeruginosa* (MIC = 7.5 mg/mL). According to Qingshan et al. (2010), antimicrobial activity increased with increase in zinc content, and with 6.28% zinc they obtained MIC of 3.5 mg/mL against *E. coli* and of 3 mg/mL against *S. aureus*, but with significantly higher MBC. According to Jiao et al. (2017), antimicrobial activity increased along with the increase in the SSA of Mnt when the size of the particles was reduced, which implied that the antimicrobial effect of Mnt did not depend only on the copper or zinc ions, but also on the surface characteristics of Mnt, as was partially confirmed by the present study (Tables 2 and 3). Using the SEM analysis, Zou et al. (2019) ascertained that growing *S. aureus* and *E. coli* in the presence of Zn-Mnt causes morphological changes manifested in a rough and distorted surface, as well as cell-membrane damage which leads, in turn, to cytoplasm leakage. According to Qingshan et al. (2010), Tan et al. (2008), and Zou et al. (2019), Zn-modified bentonite and Mnt have better antimicrobial impact on Gram-positive than Gram-negative bacteria. Those authors explained their results by the presence of the outer membrane of Gram-negative bacteria, which creates an additional protective barrier against foreign matter such as Zn-Mnt. Garshasbi et al. (2017) and Jiao et al. (2017)

https://doi.org/10.1007/s42860-023-00258-0 Published online by Cambridge University Press

stated that the zinc-modified Mnt performed better with Gram-negative bacteria due to the large negative charge of these bacteria, which enabled the contact between cells and the positively charged zinc ions. In the present experiment, the inhibiting effect of ZnB was not related to the bacteria cell wall structure. *B. cereus* was less sensitive than *E.coli*, and *P. aeruginosa* was less sensitive than *S. aureus,* probably due to the reduced sensitivity of *Bacillus* and *Pseudomonas* to heavy metals (Carpio et al., 2018; Henao & Ghneim-Herrera, 2021). The Cu/Zn-modified bentonite samples had, in most cases, a better inhibiting effect on bacteria than CuB; Cu/Zn-B1 and Cu/Zn-B2 had a better inhibiting effect than ZnB, which implied a synergistic antibacterial effect (Jiao et al., 2017; Tan et al., 2008). Based on the chemical composition (Table 1), the antibacterial activity clearly increased when ZnO and Zn were present. In the present experiment, the largest amount of ZnO and Zn was in the Cu/Zn-B2, which showed the best antibacterial effect, especially to *S. aureus.* The fact that the amount of zinc ions in Cu/Zn-B3 was greater than in ZnB, but the antibacterial activity was less, could be because of a larger SSA and smaller nanoparticles in ZnB than in Cu/Zn-B3 (Bagchi et al., 2013; da Silva et al., 2019).

Conclusions

Cu- and Zn-modified bentonite samples were prepared and characterized with ED-XRF, XRPD, SEM, FTIR, and BET analyses, and their antibacterial activity was determined by the agar dilution method against four bacteria: *Escherichia coli*, *Pseudomonas aeruginosa*, *Staphylococcus aureus,* and *Bacillus cereus*. In comparison to NaB, the greatest decrease in the textural properties was with ZnB (SP_{BET} = 6.55 m^2/g, V_p = 0.023 cm^3/g, and d = 13.41 nm), and the smallest was with Cu/Zn-B2 (SP_{BET} = 35.5 m^2/g, V_p = 0.052 cm^3/g, and d = 6.49 nm). In all samples, the value of the $SP_{ext,t}$ was much greater than the $SP_{micro,t}$; $V_{micro,t}$ was small, and in the case of ZnB and Cu/Zn-B1 it even had a negative value (below the limit of detection). ZnB and Cu/Zn-B1 had the most pronounced mesoporous character, while NB had the least pronounced mesoporous character. Modified bentonite demonstrated good antibacterial activity (except NaB) on *Escherichia coli, Pseudomonas aeruginosa, Staphylococcus aureus,* and *Bacillus cereus*. Zn-modified bentonite demonstrated a greater effect than Cu- and Na-bentonite samples, while among Cu/Zn bentonite samples, Cu/Zn-B2 had the largest antibacterial effect. Non-woven textile (NT) and knitted fabric (PL) integrated with Cu/Zn-B2 showed good antibacterial activity, but NT showed more antimicrobial activity than PT, and with an increase in the concentration of applied Cu/Zn-B2, antibacterial properties incresased. This study showed that the copper and zinc intercalated clays have a good potential as antibacterial finishing agents for textile materials.

Acknowledgments Financial support from the Ministry of Scientific and Technological Development, Higher Education and Information Society of the Republic of Srpska (Contract No.19/06-020/961-63/18) is acknowledged.

Declarations

Conflict of Interest On behalf of all authors, the corresponding author states that there is no conflict of interest.

REFERENCES

AATCC TM 147-2004. Test Method for Antibacterial Activity of Textile Materials: Parallel Streak. *AATCC Manual of International Test Methods and Procedures*.

Abdalkader, D., & Al-Saedi, F. (2020). Antibacterial effect of different concentration of zinc sulfate on multidrug resistant pathogenic bacteria. *Systematic Reviews in Pharmacy, 11*(*3*), 282–288.

Abou el-Kheir, A., El-Ghany, N. A. A., Fahmy, M. M., Aboras, S. E., & El-Gabry, L. K. (2020). Functional finishing of polyester fabric using bentonite nano-particles. *Egyptian Journal of Chemistry, 63*(*1*), 85–99. https://doi.org/10.21608/EJCHEM.2019.20404.2223

Aguzzi, C., Cerezo, P., Viseras, C., & Caramella, C. (2007). Use of clays as drug delivery systems: Possibilities and limitations. *Applied Clay Science, 36*, 22–36. https://doi.org/10.1016/j.clay.2006.06.015

Ahamed, M., Alhadlaq, H. A., Khan, M. A. M., Karuppiah, P., & Al-Dhabi, N. A. (2014). Synthesis, characterization and antimicrobial activity of copper oxide nanoparticles. *Journal of Nanomaterials, 637858*. https://doi.org/10.1155/2014/637858

Aldayel, O. A., Alandis, N. M., Mekhemer, W. K., Hefne, J. A., & Al-Raddadi, S. (2008). Zn(II) removal using natural bentonite: Thermodynamics and kinetic studies. *Material Science Research India, 5*(*1*), 25–36. https://doi.org/10.13005/msri/050104

Amir, M., Hasany, S. F., & Asghar, M. S. A. (2023). Modification of bentonite nanoclay for textile application. *Polimery, 68*(*2*), 79–85. https://doi.org/10.14314/polimery.2023.2.1

Aprile, F., & Lorandi, R. (2012). Evaluation of Cation Exchange Capacity (CEC) in Tropical Soils Using Four Different Analytical Methods. *Journal of Agricultural Science, 4*(*6*), 278–289. https://doi.org/10.5539/jas.v4n6p278

Bagchi, B., Kar, S., Dey, S. K., Bhandary, S., Roy, D., Mukhopadhyay, T. K., Das, S., & Nandy, P. (2013). In situ synthesis and antibacterial activity of copper nanoparticle loaded natural Mnt clay based on contact inhibition and ion release. *Colloids and Surfaces B: Biointerfaces, 108*, 358–365. https://doi.org/10.1016/j.colsurfb.2013.03.019

Balci, S. (2019). Structural Property Improvements of Bentonite with Sulfuric Acid Activation and a Test in Catalytic Wet Peroxide Oxidation of Phenol. *International Journal of Chemical Reactor Engineering, 17*(*6*), 20180167. https://doi.org/10.1515/ijcre-2018-0167

Balek, V., Beneš, M., Šubrt, J., Pérez-Rodriguez, J. L., Sánchez-Jiménez, P. E., Pérez-Maqueda, L. A., & Pascual-Cosp, J. (2008). Thermal characterization of Mnt clays saturated with various cations. *Journal of Thermal Analysis and Calorimetry, 92(1)*, 191–197. https://doi.org/10.1007/s10973-007-8761-9.7

Barrett, E. P., Joyner, L. G., & Halenda, P. P. (1951). The determination of pore volume and area distributions in porous substances. I. Computations from Nitrogen Isotherms. *Journal of the American Chemical Society, 73*(*1*), 373–380. https://doi.org/10.1021/ja01145a126

Begam, R., Joshi, M., & Parwar, R. (2022). Antimicrobial finishing of cotton textiles using silver intercalated clay. *Fibers and Polymers, 23*(*1*), 148–154. https://doi.org/10.1007/s12221-021-3178-9

Benhalima, L., Amri, S., Bensouilah, M., & Ouzrout, R. (2019). Antibacterial effect of copper sulfate against multi-drug resistant nosocomial pathogens isolated from clinical samples. *Pakistan Journal of Medical Sciences, 35*(*5*), 1322–1328. https://doi.org/10.12669/pjms.35.5.336

Benli, H., & Bahtiyari, M. İ. (2015). Use of ultrasound in biopreparation and natural dyeing of cotton fabric in a single bath. *Cellulose, **22***, 867–877. https://doi.org/10.1007/s10570-014-0494-x

Bhattacharya, M., Maiti, M., & Bhowmick, A. K. (2008). Influence of different nanofillers and their dispersion methods on the properties of natural rubber nanocomposites. *Rubber Chemistry and Technology, 81*(5), 782–808. https://doi.org/10.5254/1.3548232

Catovic, C., Abbes, I., Barreau, M., Sauvage, C., Follet, D.-P. C., Groboillot, A., Leblanc, S., Svinareff, P., Chevalier, S., & Feuillolley, M. G. J. (2022). Cotton and flax textiles leachables impact differently cutaneous *Staphylococcus aureus* and *Staphylococcus epidermidis* biofilm formation and cytotoxicity. *Life, 12*, 535. https://doi.org/10.3390/life12040535

Carpio, M. I. E., Ansari, A., & Rodrigues, D. F. (2018). Relationship of biodiversity with heavy metal tolerance and sorption capacity: a meta-analysis approach. *Environmental Science & Technology, 52*(*1*), 185–194. https://doi.org/10.1021/acs.est.7b04131

Caruso, M. R., Cavallaro, G., Milioto, S., Fakhrullin, R., & Lazzara, G. (2023). Halloysite nanotubes/Keratin composites for wool treatment. *Applied Clay Science, 238*, 106930. https://doi.org/10.1016/j.clay.2023.106930

Chen, M. X., Alexander, K. S., & Baki, G. (2016). Formulation and evaluation of antibacterial creams and gels containing metal ions for topical application. *Journal of Pharmaceutics, 5754349*. https://doi.org/10.1155/2016/5754349

Claudel, M., Schwarte, J. V., & Fromm, K. M. (2020). New antimicrobial strategies based on metal complexes. *Chemistry, 2*, 849–899. https://doi.org/10.3390/chemistry2040056

Clegg, F., Breen, C., Muranyi, P., & Schönweitz, C. (2019). Antimicrobial, starch based barrier coatings prepared using mixed silver/sodium exchanged bentonite. *Applied Clay Science, 179*, 105144. https://doi.org/10.1016/j.clay.2019.105144

da Silva, B. L., Abucafy, M. P., Manaia, E. B., Junior, J. A. O., Chiari-Andreo, B. G., Pietro, R. C. L. R., & Chiavacci, L. A. (2019). Relationship between structure and antimicrobial activity of zinc oxide nanoparticles: an overview. *International Journal of Nanomedicine, 14*, 9395–9410. https://doi.org/10.2147/IJN.S216204

de Araujo, A. L. P., Bertagnolli, C., da Silva, M. G. C., Gimenes, M. L., & de Barros, M. A. S. D. (2013). Zinc adsorption in bentonite clay: influence of pH and initial concentration. *Acta Scientiarum Technology, 35*(2), 325–332. https://doi.org/10.4025/actascitechnol.v35i2.13364

de Oliviera, C. R. S., Batistella, M. A., Lourenco, L. A., de Aruda, S. M., de Souza, G. U., & de Souza, A. A. U. (2021). Cotton fabric finishing based on phosphate/clay mineral by direct-coating technique and its influence on the thermal stability of the fibers. *Progress in Organic Coatings, 150*, 105949. https://doi.org/10.1016/j.porgcoat.2020.105949

DIN 53923. (2022) DE. Testing of Textiles; Determination of Water Absorption of Textile Fabrics. Berlin: Beuth Verlag.

Ezquerro, C. S., Ric, G. I., Miñana, C. C., & Bermejo, J. S. (2015). Characterization of Mnts modified with organic divalent phosphonium cations. *Applied Clay Science, 111*, 1–9. https://doi.org/10.1016/j.clay.2015.03.022

Farmer, V. C. (1974). The layer silicates. In V. C. Farmer (Ed.), *The Infrared Spectra of Minerals* (pp. 331–363). Mineralogical Society.

Gamiz, E., Linares, J., & Delgado, R. (1992). Assessment of two Spanish bentonites for pharmaceutical uses. *Applied Clay Science, 6*, 359–368. https://doi.org/10.1016/0169-1317(92)90003-6

Garshasbi, N., Ghorbanpour, M., Nouri, A., & Loffiman, S. (2017). Preparation of zinc oxide-nanoclay hybrids by alkaline ion exchange method. *Brazilian Journal of Chemical Engineering, 34*(*04*), 1055–1063. https://doi.org/10.1590/0104-6632.20170344s20150570

Gomes, C., Rautureau, M., Poustis, J., & Gomes, J. (2021). Benefits and risks of clays and clay minerals to human health from ancestral to current times: a synoptic overview. *Clays and Clay Minerals, 69*, 612–632. https://doi.org/10.1007/s42860-021-00160-7

Grujić, D., Savić, A., Topalić-Trivunović, L., Jevšnik, S., Rijavec, T., & Gorjanc, M. (2015). The influence of plasma pretreatment on the structure and antimicrobial properties of knitted fabrics treated with herbal extracts. *ACC Journal, 21*(*1*), 30–42. https://doi.org/10.15240/tul/004/2015-1-004

Hasan, K., Hridam, D., Rahman, M., Morshed, M., Al Azad, S., & Genyang, C. (2016). A review on antibacterial coloration agents activity, implementation & efficiency to ensure the ecofriendly & green textiles. *American Journal of Polymer Science & Engineering, 4*(*1*), 39–59.

Hayati-Ashtiani, M. (2012). Use of FTIR spectroscopy in the characterization of natural and treated nanostructured bentonite (Mnts). *Particulate Science and Technology, 30*(*6*), 553–564. https://doi.org/10.1080/02726351.2011.615895

Henao, S. G., & Ghneim-Herrera, T. (2021). Heavy metals in soils and the remediation potential of bacteria associated with the plant microbiome. *Frontiers of Environmental Science & Engineering, 9*, 604216. https://doi.org/10.3389/fenvs.2021.604216

Hong, R., Kang, T. Y., Michels, C. A., & Gadura, N. (2012). Membrane lipid peroxidation in copper alloy-mediated contact killing of *Escherichia coli*. *Applied and Environmental Microbiology, 78*(*6*), 1776–1784. https://doi.org/10.1128/AEM.07068-11

Horue, M., Cacicedo, M. L., Fernandez, M. A., Rodenak-Kladniew, B., Torez Sánchez, R. M., & Castro, G. R. (2020). Antimicrobial activities of bacterial cellulose – silver Mnt nanocomposites for wound healing. *Material Science and Engineering: C, 116*, 111152. https://doi.org/10.1016/j.msec.2020.111152

Hu, C.-H., & Xia, M.-S. (2006). Adsorption and antibacterial effect of copper-exchanged montmorillonite on *Escherichia coli* K88. *Applied Clay Science, 31*(*3-4*), 180–184. https://doi.org/10.1016/j.clay.2005.10.010

Ishida, T. (2017). Bacteriolyses of bacterial cell walls by Cu(II) and Zn(II) ions based on antibacterial resultss of dilution medium method and halo antibacterial tests. *Journal of Advanced Research in Biotechnology, 2*(*2*), 1–12. https://doi.org/10.15226/2475-4714/2/200120

Ivankovic, T., Rajic, A., Ercegovic Razic, S., Rolland du Roscoat, S., & Skenderi, Z. (2022). Antibacterial properties of non-modified wool, determined and discussed in relation to ISO 20645:2004 standard. *Molecules, 27*, 1876. https://doi.org/10.3390/molecules27061876

Javadhesari, S. M., Alipour, S., Mohammadhejad, S., & Akbarpour, M. R. (2019). Antibacterial activity of ultra-small copper oxide (II) nanoparticles synthesized by mechanochemical processing against *S.aureus* and *E. coli*. *Materials Science & Engineering C, 105*, 110011. https://doi.org/10.1016/j.msec.2019.110011

Jiao, L., Lin, F., Cao, S., Wang, C., Wu, H., Shu, M., & Hu, C. (2017). Preparation, characterization, antimicrobial and cytotoxicity studies of coper/zinc-loaded Mnt. *Journal of Animal Science and Biotechnology, 8*, 27. https://doi.org/10.1186/s40104-017-0156-6

Joshi, M., Ali, S. W., Purwar, R., & Rajendran, S. (2009). Ecofriendly antimicrobial finishing of textiles using bioactive agents based on natural products. *Indian Journal of Fibre and Textile Research, 34*(*3*), 295–304.

Jović-Jovičić, N. P., Milutinović-Nikolić, A. D., Gržetić, I. A., Banković, P. T., Marković, D. M., & Jovanović, B. Ž. (2008). The influence of modification on structural textural and adsorption properties of bentonite. *Hemijska Industrija, 62*(3), 131–137. https://doi.org/10.2298/HEMIND0803131J

Kalia, A., Abd-Elsalam, K., & Kuca, K. (2020). Zinc-based nanomaterials for diagnosis and management of plant diseases: ecological safety and future perspective. *Fungi, 6*(*4*), 222. https://doi.org/10.3390/jof6040222

Kaya, A., & Ören, A. H. (2005). Adsorption of zinc from aqueous solutions to bentonite. *Journal of Hazardous Materials, B125*, 183–189. https://doi.org/10.1016/j.jhazmat.2005.05.027

Kertman, N., Dalbaşi, E. S., Körlü, A., Özgüney, A. T., & Yapar, S. (2020). A study on coating with nanoclay on the production of flame retardant cotton fabrics. *Tekstil ve Konfeksiyon, 300*, 4. https://doi.org/10.32710/tekstilvekonfeksiyon.675352

Kozák, O., Praus, P., Machovič, V., & Klika, Z. (2010). Adsorption of zinc and copper ions on natural and ethylenediamine modified Mnt. *Ceramics – Silikáty, 54*(*1*), 78–84.

Kumar, A. & Lingfa, P. (2019). Physicochemical characterization of sodium bentonite clay and its significance as a catalyst in plastic waste valorization. In *3rd International Conference on Electronics, Materials Engineering & Nano Technology (IEMENTech)* (pp. 1–4). https://doi.org/10.1109/IEMENTech48150.2019.8981195

Lippens, B. C., & de Boer, J. H. (1965). Studies on pore systems in catalysts: V. *The t method. Journal of Catalysis, 4*(*3*), 319–323. https://doi.org/10.1016/0021-9517(65)90307-6

Lisuzzo, L., Cavallaro, G., Milioto, S., & Lazzara, G. (2021). Halloysite nanotubes filled with MgO for paper reinforcement and deacidification. *Applied Clay Science, 213*, 106231. https://doi.org/10.1016/j.clay.2021.106231

Madejová, J. (2003). FTIR techniques in clay mineral studies. *Vibrational Spectroscopy, 31*, 1–10. https://doi.org/10.1016/S0924-2031(02)00065-6

Magana, S. M., Quintana, P., Aguilar, D. H., Toledo, J. A., Angeles-Chavez, C., Cortes, M. A., Leon, L., Freile-Pelegrin, Y., Lopez, T., & Torres Sanchez, R. M. (2008). Antibacterial activity of Mnts modified with silver. *Journal of Molecular Catalysis A: Chemical, 281*, 192–199. https://doi.org/10.1016/j.molcata.2007.10.024

Martsouka, F., Papagiannopoulos, K., Hatziantoniou, S., Barlog, M., Lagiopoulos, G., Tatoulis, T., Tekerlekopoulou, A. G., Lampropoulou, P., & Papoulis, D. (2021). The antimicrobial properties of modified pharmaceutical bentonite with zinc and copper. *Pharmaceutics, 13*(*8*), 1190. https://doi.org/10.3390/pharmaceutics13081190

Németh, T., Mohai, I., & Tóth, M. (2005). Adsorption of copper and zinc ions on various Mnts: an XRD study. *Acta Mineralogica-Petrographica, 46*, 29–36.

Ning, C., Wang, X., Li, L., Zhu, Y., Li, M., Yu, P., Zhou, L., Zhou, Z., Chen, J., Tan, G., Zhang, Y., Wang, Y., & Mao, C. (2015). Concentration ranges of antibacterial cations for showing the highest antibacterial efficacy but the least cytotoxicity against mammalian cells: implications for a new antibacterial mechanism. *Chemcal Research.*

Toxicology, 21, 28(9), 1815–1822. https://doi.org/10.1021/acs.chemrestox.5b00258

Ortez, J. H. (2005). Disk diffusion testing. In M. B. Coyle (Ed.), *Manual of Antimicrobial Susceptibility Testing* (pp. 39–53). American Society for Microbiology.

Paetzold, O. H., & Wiese, A. (1975). Experimentelle untersuchungen über die antimikrobielle wirkung von zinkoxid. *Archives of Dermatological Research, 253*, 151–159. https://doi.org/10.1007/BF00582067

Pajarito, B. B., Castañeda, K. C., Jeresano, S. D., & Repoquit, D. A. (2018). Reduction of Offensive Odor from Natural Rubber Using Zinc-Modified Bentonite. *Advances in Materials Science and Engineering, ID, 9102825*. https://doi.org/10.1155/2018/9102825

Parolo, M. E., Fernández, L. G., Zajonkovsky, I., Sánchez, M. P., & Baschini M.(2011). Antibacterial activity of materials synthesized from clay minerals. In: Mendez-Vilas, A., *Science against microbial pathogens: communicating current research and technological advances*. Formatex Research Center, pp.144-151

Pasquet, J., Chevalier, Y., Pelletier, J., Couval, E., Bouvier, D., & Bozinger, M.-A. (2014). The contribution of zinc ions to the antimicrobial activity of zinc oxide. *Colloids and Surfaces A: Physicochemical and Engineering Aspects, 457*(*1*), 263–274. https://doi.org/10.1016/j.colsurfa.2014.05.057

Pazourková, L., Reli, M., Hundáková, M., Pazdziora, P., & D., Martynková, G.S., & Lafdi, K. (2019). Study of the Structure and antimicrobial Activity of Ca-Deficient Ceramics on Chlorhexidine Nanoclay Substrate. *Materials, 12*, 2996. https://doi.org/10.3390/ma12182996

Pejon, O. J. (1992). *Mapeamento geotécnico da folha de Piracicaba-SP (escala 1:100.000): estudo de aspectos metodológicos, de caracterização e de apresentação dos atributos*. Departamento de Geotecnia, Escola de Engenharia de São Carlos, USP, São Carlos, 2v. 224 pp. (Thesis)

Petrović, R., Levi, Z., & Penavin-Škundric, J. (2019). Adsorpcija amonijum jona i amonijaka iz vodene sredine na bentonitu i mordenitu. *Glasnik Hemičara Tehnologa I Ekologa Republike Srpske, 15*, 1–8. https://doi.org/10.7251/GHTE1915001P

Petrovic, Z., Dugic, P., Aleksic, V., Begic, S., Sadadinovic, J., Micic, V., & Kljajic, N. (2014). Composition, structure and textural characteristics of domestic acid activated bentonite. *Contemporary Materials, V-I, 133–39*. https://doi.org/10.7251/cm.v1i5.1509

Pourabolghasem, H., Gharbanpour, M., & Shayegh, R. (2016). Antibacterial activity of copper-doped Mnt nanocomposites prepeared by alkaline ion exchange method. *Journal of Physical. Science, 27*(2), 1–12. https://doi.org/10.21315/jps2016.27.2.1

Qingshan, S., Shaozao, T., Quihui, Y., Zepeng, J., Yousheng, O., & Yiben, C. (2010). Preparation and characterization of antibacterial Zn^{2+} - exchanged Mnts. *Journal of Wuhan University of Technology-Materials Science Edition, 94397212*. https://doi.org/10.1007/s11595-010-0080-5

Rather, W., Muhee, A., Bhat, R. A., Ul Haq, A., Nubi, S. U., Malik, H. U., & Taifa, S. (2020). Antimicrobial activity of copper sulphate and zinc sulphate on major mastitis causing bacteria in cattle. *The Pharma Innovation Journal, 9*(*4*), 93–95.

Ranđelović, M. S., Purenović, M. M., Matović, B. Z., Zarubica, A. R., Momčilović, M. Z., & Purenović, J. M. (2014). Structural, textural and adsorption characteristics of bentonite-based composite. *Microporous and Mesoporous Materials, 195*, 67–74. https://doi.org/10.1016/j.micromeso.2014.03.031

Roy, A., & Joshi, M. (2018). Enhancing antibacterial properties of polypropylene/Cu-MMT nanocomposites filaments through sheath-core morphology. *Polymer International, 67*(*7*), 917–924. https://doi.org/10.1002/pi.5580

Russell, J. D., & Farmer, V. C. (1964). Infra-red spectroscopic study of the dehydration of montmorillonite and saponite. *Clay Minerals Bulletin, 5*(*32*), 443–464. https://doi.org/10.1180/claymin.1964.005.32.04

Sadhu, S. D., & Bhowmick, A. K. (2004). Preparation and properties of styrene–butadiene rubber based nanocomposites: The influence of the structural and processing parameters. *Journal of Applied Polymer Science, 92*, 698–709. https://doi.org/10.1002/app.13673

Şahiner, A., Özdemir, G., Bulut, T. H., & Yapar, S. (2022). Synthesis and Characterization of Non-leaching Inorgano- and Organo-montmorillonites and their Bactericidal Properties Against *Streptococcus mutans*. *Clays and Clay Minerals, 70*, 481–491. https://doi.org/10.1007/s42860-022-00198-1

Sanchez-Lopez, E., Gomes, D., Esteruelas, G., Bonilla, L., Lopez-Machado, A. L., Galindo, R., Cano, A., Espinia, M., Ettcheto, M., Camins, A., Silva, A. M., Durazzo, A., Santini, A., Garcia, M. L., & Souto, E. B. (2020). Metal-based nanoparticles as antimicrobial agents: an overview. *Nanomaterials, 10*(*2*), 292. https://doi.org/10.3390/nano10020292

Söderberg, T. A., Sunzel, B., Holm, S., Elmros, T., Hallmans, G., & Sjöberg, S. (1990). Antibacterial Effect of Zinc Oxide in Vitro. *Scandinavian Journal of Plastic and Reconstructive Surgery and Hand Surgery, 24*(*3*), 193–197. https://doi.org/10.3109/02844319009041278

Stodolak-Zych, E., Kurpanik, R., Dzierzkowska, E., Gajek, M., Zych, K., Gryn, K., & Rapacz-Kmita, A. (2021). Effect of Mnt and gentamicin addition on the properties of electrospun polycarpone fibers. *Materials, 14*, 6905. https://doi.org/10.3390/ma14226905

Sugarman, B. (1983). Zinc and infection. *Reviews of Infectious Diseases, 5*, 138–147. https://doi.org/10.1093/clinids/5.1.137

Surjawidjaja, J. E., Hidayat, A., & Lesmana, M. (2004). Growth inhibition of enteric pathogens by zinc sulfate: An in vitro study. *Medical Principles and Practice, 13*, 286–289. https://doi.org/10.1159/000079529

Tan, S.-Z., Zhang, K.-H., Zhang, L.-L., Xie, Y.-S., & Liu, Y.-L. (2008). Preparation and characterisation of the antibacterial Zn^{2+} or/and Ce^{3+} loaded montmorillonites. *Chinese Journal of Chemistry, 26*(*5*), 865–869. https://doi.org/10.1002/cjoc.200890160

Tong, G., Yulong, M., Peng, G., & Zirong, X. (2005). Antibacterial effects of the Cu(II)-exchanged montmorillonite on

Escherichia coli K88 and *Salmonella choleraesuis*. *Veterinary Microbiology, 105*(*2*), 113–122. https://doi.org/10.1016/j.vetmic.2004.11.003

Toor, M. K. (2010). *Enhancing adsorption capacity of bentonite for dye removal: Physiochemical modification and characterization*. *Masters Thesis*,. University of Adelaide.

Tyagi, B., Chudasama, C. D., & Jasra, R. V. (2006). Determination of structural modification in acid activated Mnt clay by FT-IR spectroscopy. *Spectrochimica Acta Part A: Molecular and Biomolecular Spectroscopy, 64*(*2*), 273–278. https://doi.org/10.1016/j.saa.2005.07.018

Uddin, F. (2013). Studies in finishing effects of clay mineral in polymers and synthetic fibers. *Advances in Material Science and Engineering, 243515*. https://doi.org/10.1155/2013/243515

VDG P69. (1999). *Bindemittelprüfung - Prüfung von Bindetonen*. *Technical report*.

Vuković, Z., Milutinović-Nikolić, A., Krstić, J., Abu-Rabi, A., Novaković, T., & Jovanović, D. (2005). The Influence of Acid Treatment on the Nanostructure and Textural Properties of Bentonite Clays. *Materials Science Forum, 494*, 339–344. https://doi.org/10.4028/www.scientific.net/msf.494.339

Williams, L. B. (2019). Natural antibacterial clays: historical uses and modern advances. *Clays and Clay Mineral, 67*, 7–24. https://doi.org/10.1007/s42860-018-0002-8

Wilson, S. A., Laing, R. M., Tan, E., Wilson, C. A., Arachchige, P. S. G., Gordon, K. C., & Fraser-Miller, S. J. (2023). Determining deposits on knit fabrics, yarns, and fibers, from sensor-related treatments. *The Journal of The Textile Institute*. https://doi.org/10.1080/00405000.2023.2221427

Zou, Y.-H., Wand, J., Cui, L.-Y., Zeng, R.-C., Wand, Q.-Z., Han, Q.-X., Qiu, J., Chen, X.-B., Chen, D.-C., Guan, S.-K., & Zheng, Y.-F. (2019). Corrosion resistance and antibacterial activity of zinc-loaded Mnt coatings on biodegradable magnesium alloy AZ31. *Acta Biomaterialia, 98*, 196–214. https://doi.org/10.1016/j.actbio.2019.05.069